Comparison of Experimental and Numerical Heat Losses on Air Conditioned Office in Desert Climate

Ali M. Wahhad[1], Nor Mariah Adam[1], Mohd S.Salit[1], and Ahmed A.B. Alarabi[2*]

[1]Mechanical and Manufacturing Engineering Department, Putra University Malaysia, Malaysia
[2*] College of Engineering Technology, Hoon, Libya
    Bohmaid2000@yahoo.com

Abstract

In recent years, the building community has integrated sustainable design concepts that can improve indoor air quality while conserving energy in buildings. A computational fluid dynamics (CFD) simulation program using three-dimensional flow finite difference of k –ε has been used and compared with experimental results. The study was carried in a new air-conditioned administrative office center built in 2002 as part of Libya's regional development, as shown in Figure 1. The building is located in Hoon City, province of Al Jufrah, Southern Libya, at lat. 7' N and lat. 56' E. Experimentally eight thermocouples were placed at eight different positions on the inner surface to measure the surface inner temperature. The main aim of the study is to evaluate the temperature difference between outdoor and indoor and the distribution of the air temperature and the velocity inside the room. The temperature differences between the indoor and outdoor was found to be varied between 9 °C to15 °C. Good agreement was achieved between the computed and measured results. The error percentage was varied from 0.3% to 0.8%. For both inner and outer surface, good agreement between experimental and CFD heat transfer coefficient has been achieved.

Keywords: Double-glazed window, new model office building, desert climate, CFD, heat transfer coefficient.

Nomenclature:

N	number of hexahedron cells
a	grid spacing
n	number of nodes
ρ	density of fluid
t	time
u	velocity magnitude in x direction
v	velocity magnitude in y direction
w	velocity magnitude in z direction
τ	shear stress
$C_{i\epsilon}$	constants used in turbulent model
σ_k	turbulent Prandtl numbers for k
σ_E	turbulent Prandtl numbers for e

E total energy

$(\tau_{ij})_{eff}$ deviatory stress tensor

T temperature

c_p specific heat capacity at constant pressure

C_{ij} convection term in Reynolds stress transportation equation

D_{ij}^T turbulent diffusion term in Reynolds stress transportation equation (RSTE)

D_{ij}^L molecular diffusion term in RSTE

P   pressure

e internal energy

k turbulent kinetic energy

ε rate of dissipation

μ_t turbulent viscosity

G_k generation of turbulent kinetic energy resulting from mean velocity gradients

I number of iterations

Y_M contribution of fluctuating dilatation in turbulence to overall dissipation rate

1. Introduction

1.1 Building Description

The chosen building consists of four storeys. The building is an air-conditioned administrative office center built in 2002 as part of Libya's regional development, as shown in Figure 1. The building is located in Hoon City, province of Al Jufrah, Southern Libya, at lat. 29^0 7' N and lat. 15^0 56' E, 300 km south of the Mediterranean coast.
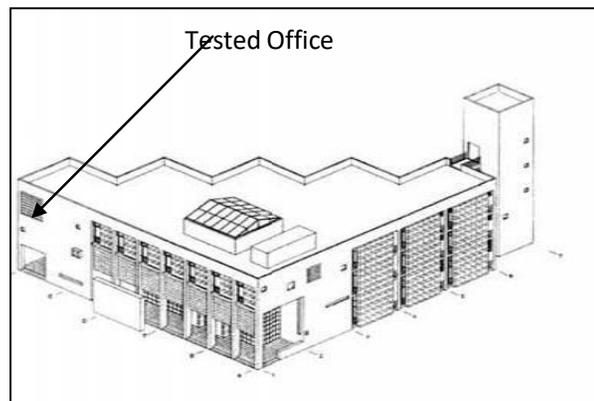
Figure 1. Building model sketch

The glazing window is weakest in an office barrier against heat transfer compared with solid exterior walls during the solar radiation and the difference in temperature between the internal and the external passage of the environment. Double glazed window is considered the most widely used today in modern buildings, which are sufficient to improve the energy through the use of low-emission devices coating to reduce heat radiation losses [1]. The desert climate is characterized by the most extreme climatic conditions in the country. This climate sometimes characterized by high air temperature, high solar radiation, low rainfall, low humidity, and sandstorms. Direct radiation falling on and through the transparent surfaces on a building creates disproportionate amounts of energy to the heat balance of the building [2]. The purpose of most air conditioning systems is to provide comfort and better air quality in enclosed places, especially in desert areas where the weather is characterized by high temperatures and low humidity, sand storms sometimes. Windows are often among the largest sources of unwanted heat gain in the desert summer climate. Large double-glazing windows have been installed as a part of the modern office design in the desert area. Computational fluid dynamics (CFD) was used broadly in order to gain insight into this issue, but the choice of models suitable for radiation, convection and the effects of turbulence remains a major challenge. Over the past two decades, computational fluid dynamics (CFD) has become a useful tool for designers to investigate the circumstances of the internal and external environment in building designs. The CFD technique has been successfully applied in building design, enabling designers to analyze the flow pattern of the air conditioning system within a short period of time, a task that was previously impossible in experimental and theoretical methods [3]. Moreover, CFD helps to determine the actual distribution of air flow, temperature, and humidity in the entire domain, which is challenging to obtain from the experiments because of time and cost factors. Unfortunately, no universal model represents the full flow pattern and flow of the air conditioning system [4]. Baker AJ et al., evaluated thermal comfort conditions of an air-conditioned lecture theater using measurement via CFD modeling.

The simulation, prediction and evaluation have become today one of the issues of modern natural ventilation, air conditioning engineering research and design of indoor and

outdoor air environment. It is a scientific and effective by using CFD numerical prediction, simulation and evaluation, and taken more seriously. K.W.D. Cheong et al., were used the PHOENICS to continue in 3D simulation for indoor environment [6]. María José Suárez et al., presented a three-dimensional numerical simulation (CFD) of the airflow inside the glazing gallery [7]. They reported that the behavior was closely linked to the weather conditions (irradiation and outdoor temperature), the high degree of radiation, outdoor temperature values, the more energy can be collected in the gallery. Jorge S. Carlos et al., presented a mathematical model based on heat transfer expressions for ventilated double window to predict thermal performance of design and parameter conditions [8]. They showed that the energy of the delivered air is influenced by the temperature difference between indoors and outdoors, by incident solar radiation and airflow rate. Kamal A.R et al., were investigated three types of windows concerning a numerical simulation for hot climates. The tested windows were a single glass window, double glass window filled with absorbing gases and ventilated double glass window [9]. The numerical simulations were realized with three mixtures of gases, a strongly absorbing gas mixture, an intermediate absorbing gas mixture and a transparent to infrared radiation mixture. The double glass window filled with absorbing gas and absorbing glass sheets was the most effective. Sujoy Pal et al., developed mathematical models to simulate the window plane solar radiation and corresponding glazing surface temperature aiming at validating the measured values. They were predicted the thermal performance of building interior due to the impact of solar radiation [10]. Ooi Yongsona et al., analyzed temperature and velocity distribution over various virtual planes for different locations of the air conditioner blower to achieve the maximum comfort for the occupant. K–epsilon and Reynolds stress models for turbulence flow were used for the analysis. The simulation of Reynolds stress model took a longer time compared to the k–epsilon model, but mesh spacing independency seem to be more significant [11]. Sami A. Al-Sanea et al., have offered air flow and thermal characteristics in air-conditioned rooms under conditions of turbulent mixed convection. Air velocity and temperature distributions were determined by CFD model and compared with experimental results [12]. Murakami S. et al., analyzed and proved that the validity of the thermal

environment in the indoor model based on turbulent flow, such as K-ε model, standard, was to be fairly accurate [13]. H.B. Awbi et al. measured the thermal air velocity and temperature distributions in a test room and compared the results with the 2-Dfinite-volume method (K-ε) model, and good agreement has been achieved. [14].

The numerical prediction of interactions between indoor and outdoor thermal environments has focused by a number of previous studies [15-22].

2. Interior Design Description

The testing office is located on the third floor of a four-storeys reinforced concrete building. The office is 4.5 m long × 3.80 m wide × 3.20 m high, as shown in Figure 2. The external walls is made up of concrete consisting of two sides, each side with thickness of 20 cm between them is a polyurethane with foam the thickness of 5 cm to prevent heat entrance inside the office. A double vertical glass overlooking the northern facade of the building is found. Dimensions of the glass was 2.36 m length x 2.36 m width x 6 mm thickness for each layer. The space between the two glass surfaces is 20 mm. The east and north walls are exterior walls, and the west and south walls are interior. The exterior walls are doubled walls with 20 cm thickness. The space between the walls is filled with polyurethane foam, an isolating material with 5 cm thickness, while the office floor is covered with a marble material. The walls are painted with a white color. An air-conditioner blower has been installed symmetrically in the office and is positioned on the southern wall. The distance between the air conditioner and both the ceiling and ground is 0.15 and 3 m, respectively. The room is illuminated by three sets of twin double-batten fluorescent lights.

The aim of the present study is to evaluate the internal distribution of air temperatures starting from the window up to the center of the room. This study also intends to evaluate the temperature difference between outdoor and indoor environments of the office during the day.
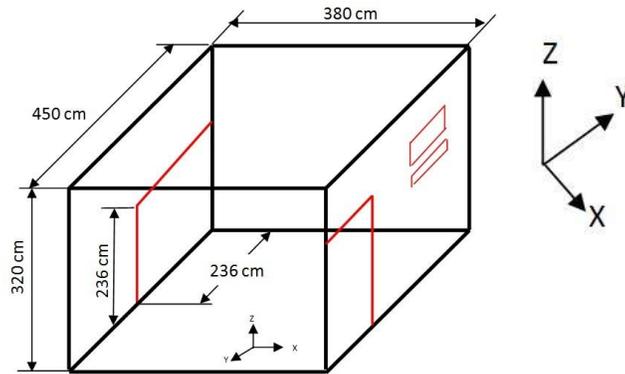
Figure 2. Office room model sketch
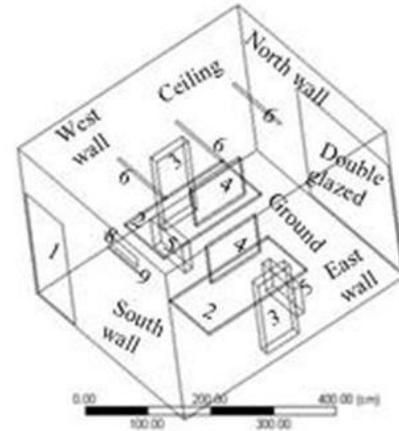
Figure 3. Surface boundary condition of test office

3. CFD Modeling and Simulation

The study involves modeling and simulation to solve fluid dynamic problems using CFD in three dimensions (3D). The ANSYS CFD V.13.0, solver FLUENT was used to simulate temperature distribution and air flow in air-condition office. The flow simulation was conducted based on the standard K-ε model [23, 24]. The flow was assumed to be three-dimensional, steady-state, incompressible, and turbulent. The air was considered as an ideal gas, and convective heat transfer at the walls and windows was calculated. The heat transfer through the large window was computed using the outside air temperature as reference, assuming steady constant heat transfer, and neglecting heat accumulation. The procedure required setting the boundary and volume conditions of the simulated module. The model was assumed to be a simple office exposed to sun rays. Boundaries should have both convection and radiation heat transfer through the window. To analyze the radiation heat transfer of mutual reflection, Monte Carlo method and Gebhart absorption coefficient method were used to calculate the factor display. The

window was set to have emissivity for outer (E-low) and inner layers (clear glass). Table 1 shows the volume condition properties of the materials.

Table 1. Volume condition properties of materials [25]

Materials	Air	Glass	Aluminum
Density (kg/m3)	1.225	2800	2719
Specific heat (J/kg 1C)	1006.43	750	871
Thermal conductivity (W/m 1C)	0.0242	0.7	177
Inner clear glass 6 mm		0.89	-
Outer (E-low), glazed (6mm)	-	0.022	-

3.1 Boundary Conditions and Meshed Domain of CFD model

The CFD model boundary conditions were provided by the experimental measurements of the wall temperatures. Figure 3 shows the surface boundary conditions used in the CFD simulation based on the experimental work. The summary of indoor loads in the testing office is reported in Table 2. The volume conditioner properties of the blocks are shown in Table 3. The walls of the office are flat. The temperature of the west, east, south, and north walls are 23.1 °C, 21.8 °C, 23.3 °C, and 20.8 °C, respectively. The heat transfer of ceiling and floor are neglected. The outer heat transfer coefficient through the window was estimated at 1.8 to 2.2 w/m^2 k.

Table 2. Indoor loads in test office

Code	ANSYS-FLUENT 13.0
Turbulence model	Standard k-ε model
Algorithm	Steady state (SIMPLE)
Analyzed area	4.5 m × 3.80 m × 3.20 m & glass Window 2.36 m x 2.36 m x 0.32 m
Convection term scheme	QUICK
Wall boundary condition	Standard log-low, adiabatic
Cells of mesh	806329

Table 3. Volume conditioner setting for properties of blocks

NO	Heat load type	Count	Model Type	Parameters Value
1	Door	1	Wall-close	-
2	Table	2	wall	-
3	People	2	people	2 X80 w/m²
4	Monitors	2	wall	2 X10 w/m²
5	Computers	2	blocks	2 X75w/m²
6	Fluorescent lamps(inactivated)	3	blocks	3 X120 w/m²
7	Double glazed window	1	wall	-
8	Air outlet	1	open	T=295K, V=2m/s
9	Air inlet	1	vent	T=296K

Various types of cells, such as tetrahedron, hexahedron, and prism dimensional cells, can be used for meshing. The hexahedron cell was chosen due to its homogeneity with the office model. The three types of grid spacing are 15 cm (coarse), 10 cm (medium), and 7.5 cm (fine). The non-uniform grids were used in consideration of the positions with large gradients of solution variables (air velocity and temperature). Grid refinement occurred on the window surface in the presence of heat source. Figure 4 shows independent testing results of the mesh.
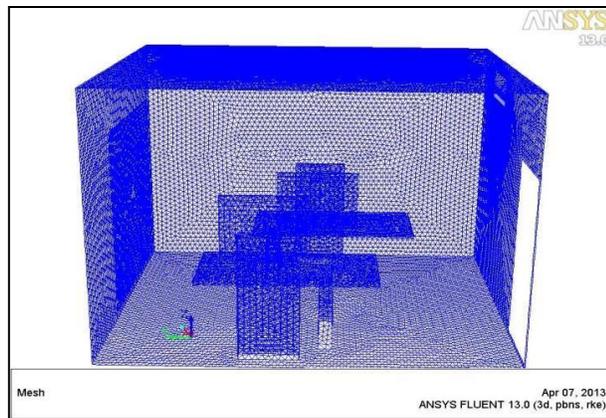
Figure 4. Grid mesh generation

3.2 Numerical simulation

The air temperature distribution patterns in the office are governed by the conservation laws of mass, momentum, and energy.

3.3 Governing equations

Three groups of basic equations are derived from the three basic laws of conservation. Mass, momentum, and energy conservation respectively result in the continuity, Navier–Stokes, and energy equations. Since turbulent flow occurs in an air-conditioned room, the k–ε and Reynolds stress viscous models have been chosen for investigation [26]. The standard k–ε model is a semi-empirical model based on model transport equations for the turbulent kinetic energy (k) and its dissipation rate (ε). The transport equation of k is derived from the exact equation, and the transport equation of ε is obtained using physical

reasoning and bears minimal resemblance to its mathematically exact counterpart. Turbulent kinetic energy (k) and its rate of dissipation (ε) are obtained from the following transport equations:

$$\frac{\partial u_i}{\partial x_i} = 0 \tag{1}$$

Where u_i is the turbulent velocity in direction x_i

$$\rho \frac{Dk}{Dt} = -\frac{\partial p}{\partial x_i}\left[\left(\mu + \frac{\mu_t}{\sigma k}\right)\frac{\partial k}{\partial x_i}\right] + G_k + G_b \, \rho\varepsilon - Y_M, \tag{2}$$

$$\rho \frac{D\varepsilon}{Dt} = -\frac{\partial p}{\partial x_i}\left[\left(\mu + \frac{\mu_t}{\sigma\varepsilon}\right)\frac{\partial \varepsilon}{\partial x_i}\right] + C_{1\varepsilon}\frac{\varepsilon}{k} + (G_k + C_{2\varepsilon}G_b) - C_{2\varepsilon}\rho\frac{\varepsilon^2}{k} \tag{3}$$

The convective heat and mass transfer modeling in the Reynolds stress models are the same as that in the k–ε model, as expressed by the following equations:

$$\frac{Dk}{Dt}(\rho E) + \frac{D}{\partial x_i}\left[(\mu_i(\rho E + P)\right] \tag{4}$$

$$\frac{\partial}{\partial x_i}\left[\left(k + \frac{c_p\mu_t}{Pr_t}\right)\frac{\partial T}{\partial x_i}\right) + u_j(\tau_{ij})_{eff}\right] + S_h \tag{5}$$

Abandoning the isotropic eddy-viscosity hypothesis, the Reynolds stress model (RSM) closes the Reynolds-averaged Navier–Stokes equations by solving transport equations of the Reynolds stresses with an equation for the dissipation rate. Therefore, four additional transport equations are required in two-dimensional flows. Seven additional transport equations must be solved in three-dimensional flows. Since the RSM accounts for the effects of streamline curvature, swirl, rotation, and rapid changes in strain rate more rigorously than on equation and two-equation models, the RSM has greater potential to provide accurate predictions for complex flows. The exact transport equations for the transport of the Reynolds stresses, $\rho\mu_i\mu_j$, may be written as follows:

$$\frac{\partial}{\partial_t}\left(\rho\mu_i\mu_j\right) + C_{ij} = D_{ij}^T + D_{ij}^L + G_{ij} + \emptyset_{ij} + \varepsilon_{ij} + F_{ij} \tag{6}$$

The turbulent kinetic energy, k, and its rate of dissipation, ε, are obtained from the following transport equations:

$$\rho \frac{DK}{Dt} = -\frac{\partial}{\partial x_j}\left[\left(\mu + \frac{\mu_t}{\sigma k}\right)\frac{\partial k}{\partial x_j}\right] + \frac{1}{2}\left(P_{ij} + G_{ij}\right) - \rho\varepsilon\,(1 + 2M_t^2), \tag{7}$$

$$\rho \frac{D\varepsilon}{Dt} = -\frac{\partial}{\partial x_j}\left[\left(\mu + \frac{\mu_t}{\sigma\varepsilon}\right)\frac{\partial \varepsilon}{\partial x_j}\right] + C_{\varepsilon 1}\frac{1}{2}\left[P_{ij} + G_{ij}\right]\frac{\varepsilon}{k} - C_{\varepsilon 2\rho}\frac{\varepsilon^2}{k}, \tag{8}$$

$$\frac{D k}{Dt}(\rho E) + \frac{D}{Dx_i}\left[\left(\mu_i(\rho E + P)\right]\right. \tag{9}$$

$$\frac{\partial}{\partial x_i}\left[\left(k + \frac{c_p\,\mu_t}{Pr_i}\right)\frac{\partial T}{\partial x_i}\right) + u_j\left(\tau_{ij}\right)_{eff}\right] + S_h \tag{10}$$

Initial and boundary conditions must be specified around the system boundary (domain) to solve these equations. The equations are highly nonlinear and cannot be solved by explicit, closed-form analytical methods. The numerical finite volume method in Fluent has been used to solve these equations. Upon solving them, the values of the dependent variables are known at the nodal points. The values of several constants in the differential equations are empirical constants at $C_{\varepsilon 1} = 1:44$ and $C_{\varepsilon 2} = 1.92$, σ_k and σ_ε are turbulent Prandtl numbers for *k* and ε, where $\sigma_k = 1.0$ and σ_ε 1.3. All slandered values were used for simulation.

4. Discussion and Recommendation

The CFD simulation package used in this study is version 13. To obtain simulated results using the CFD software, we conducted the following simulation procedure.

4.1 Temperature distribution within office.

Figure 5 shows the average temperature distribution in the office using CFD simulation. Temperature stratification, which covered almost the entire office, and average temperatures, were determined to be 25 ºC to 26 ºC within the office. The temperature difference between the outdoor and indoor environments was approximately 6 ºC to 13 ºC. The temperature difference between the ceiling and ground was approximately 1.4 ºC. The temperature of the inner surface of the window was relatively low or roughly 26.8 ºC to 29.5 ºC . The temperature of the outer surface of the window was approximately 29 ºC

to 38 °C. The temperature difference between the outer and inner surfaces varied from 9 °C to 15 °C.

Figure 11 shows the horizontal temperature distribution from the window surface to the center of the office. Table 4 shows the temperature profiles at different positions (0.5, 1, 1.5, and 2 m) from the window during the cooling period. The temperature difference between distance 0.5 and 2 m has a maximum value of approximately 2 °C at 12 am.
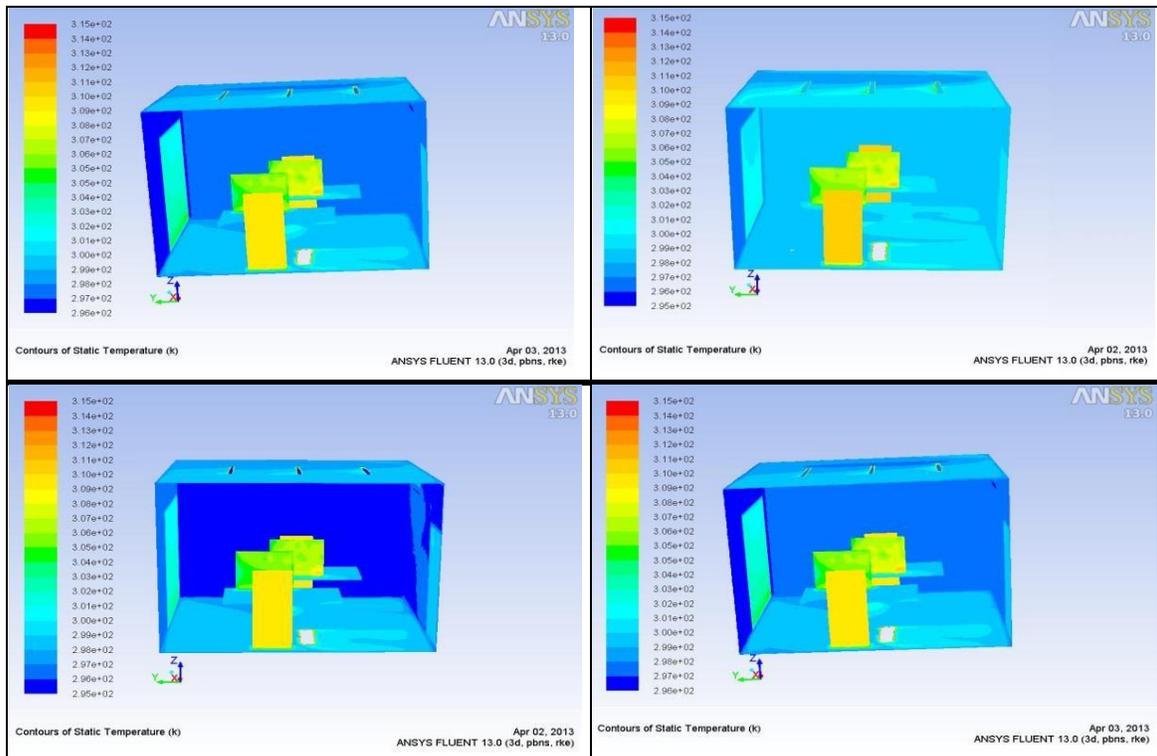
Figure 5. The average temperature distribution in the office using CFD simulation

For thermal comfort, the occupied condition was from .0.5 m to 1.5 m from the window because of the cooled air from the cooling panel of the air conditioner. In addition, the air temperature was lower near the glass window and slightly higher at a distance of 1 m from the glass window.

Table 4. Temperature distribution for distance into test office

Time	Distance			
	0.5 m	1 m	1.5 m	2 m
9:00	25.9	26	26	26.5
12:00	24.6	24.7	24.2	24.8
15:00	25.9	26	26	26.5
18:00	25.6	25.7	25.8	26.2
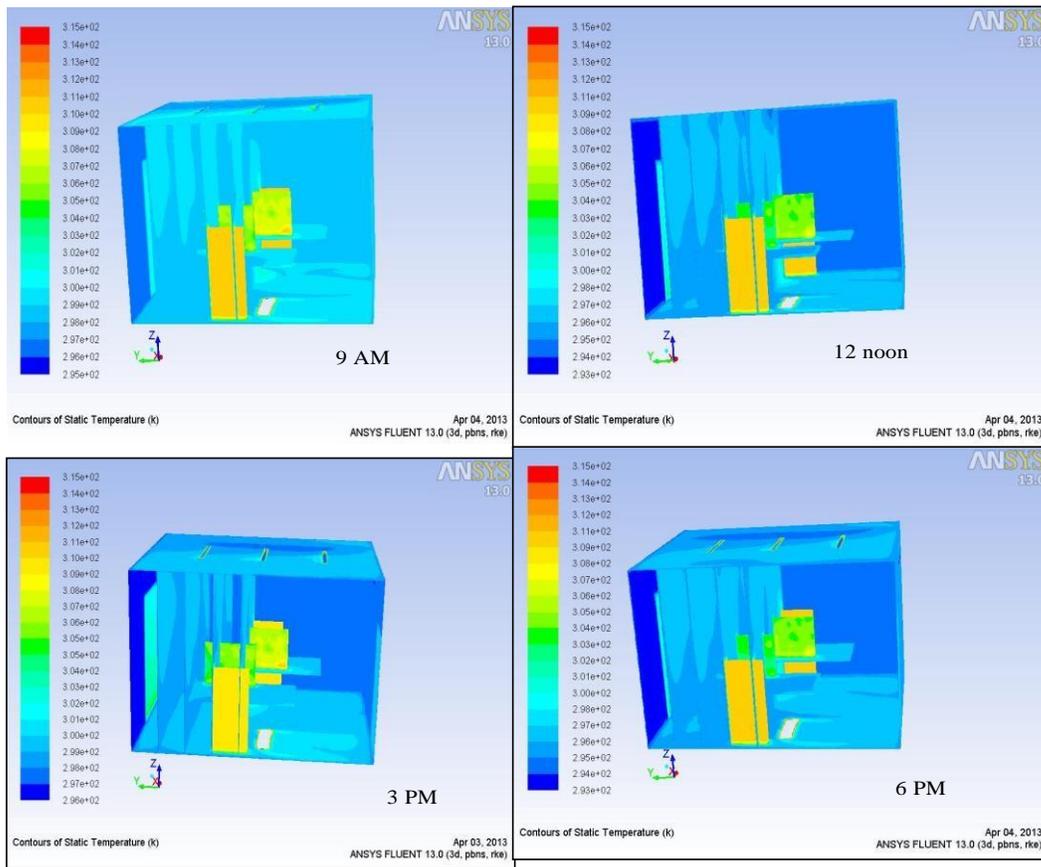
Figure 6. Temperature distribution inside the room at different time

3.2 Airflow distribution within office

Figure 7 shows the air velocity distribution in the office using CFD simulation. Air flow of velocities, which covered almost the entire office, observed that airflow near the air conditioner was 1.1 to 1.3 m/s, while a downward flow was observed close to the

windows due to emitted heat, and airflow velocity was low less than 0.3 m/s

5. Experimental Set-up Tests and Results Analysis

The experimental measurements were conducted from July to August 2009. The continuous data collection was carried out from 09:00 to 18:00. A total of 12 thermocouples were placed at different positions inside the room to measure the air and wall temperatures. The used thermocouple wires were identified as T type. The outdoor measurements and indoor air temperature was measured at the center of the office (2 m) from the window [27]. The data acquisition system of a programmable data loggers (D80 and 85) was used with online transferring. The system is illustrated in Figures 8.
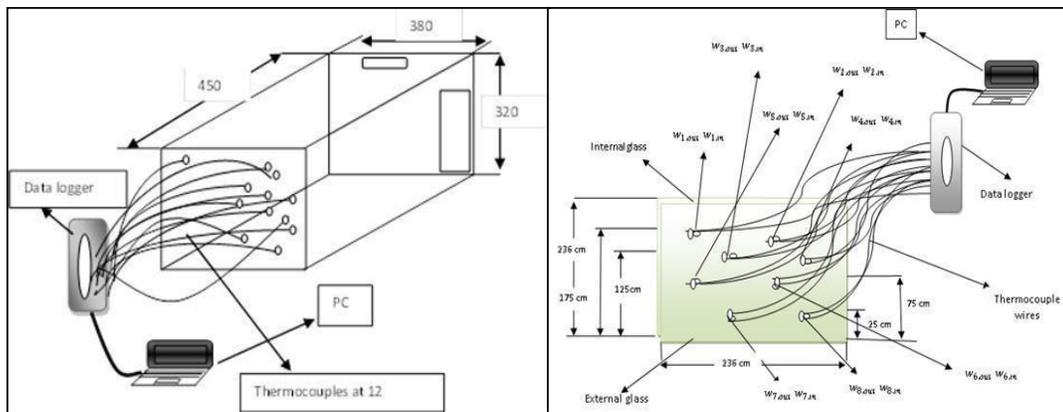
Figure 8. Thermocouples locations in the office and above external and internal surfaces of double-glazed window
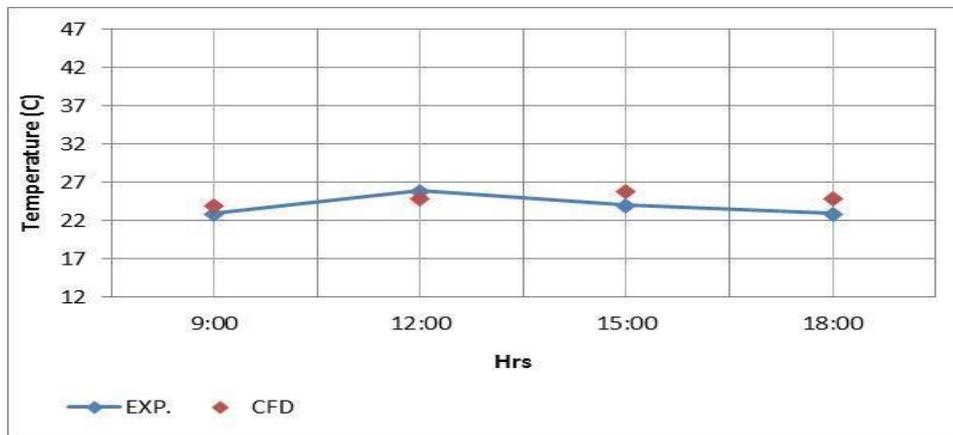
Figure 9. Comparison of variation of internal temperature with time for experimental and CFD results

The arrangements of temperature measurement are as follows: eight thermocouples were placed at eight different positions on the inner surface to measure the surface inner temperature. An additional eight thermocouples were placed on the outer surface to measure the surface outer temperature. The experimental results were compared with the theoretical (CFD simulation) to determine how they would match. Figure 9 shows the comparison average temperature inside the room. Significant agreement was achieved between the theoretical and experimental values. The average relative error varied from 0.3% to 0.7%, which was acceptable for engineering applications.

Figure 10 shows the comparison of results of the average air temperature profiles of internal and external window surfaces for both experimental and theoretical (CFD simulation) procedures. The highest temperatures of the inner surfaces was 300 K recorded At 12 noon and 15 pm.
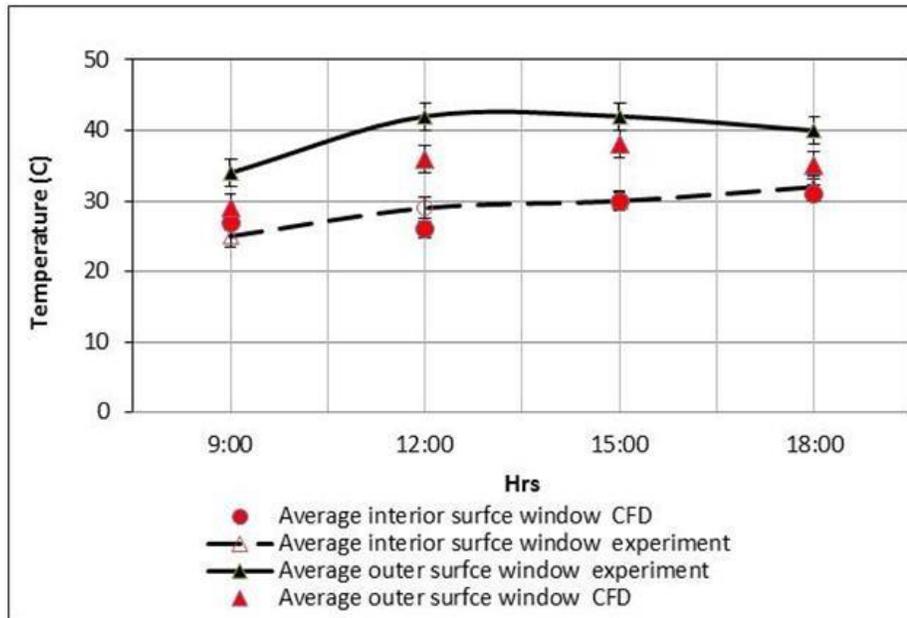
Figure 10. Comparison of experimental and CFD results of inner and outer glass surfaces

Figure 11 presents a comparison of the temperature difference between outdoor and indoor environments for the experimental and theoretical (CFD simulation) procedures. At 12 noon, only one mark appeared because of the applicability of the experimental

result to the theoretical result, such as the occurrence of overlapping. The highest temperature difference was obtained at 15:00 pm.
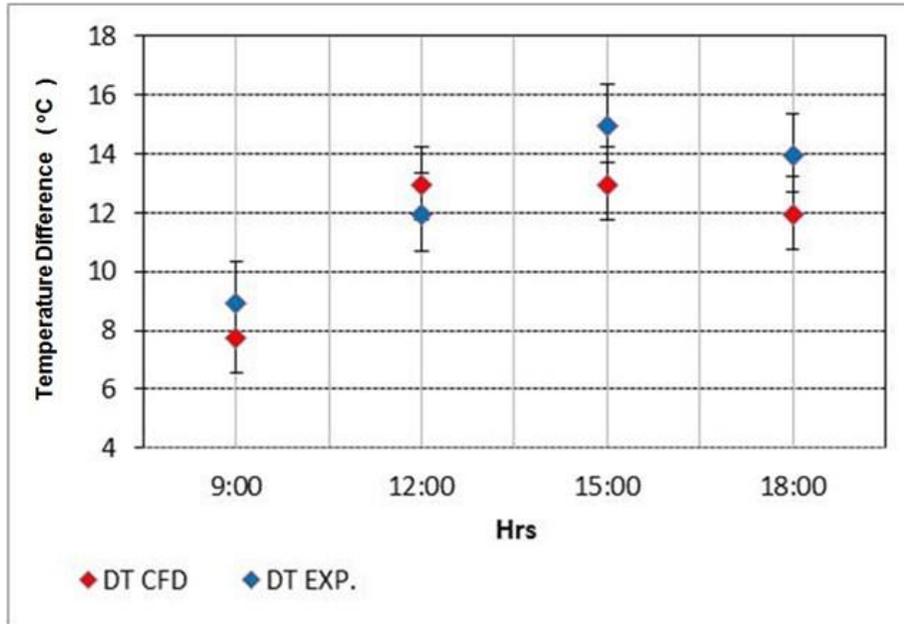
Figure 11 Comparison of experimental and CFD results of temperatures difference between outdoor and indoor environments of office

Figure 12 shows the variation of inner heat transfer coefficient from 9:00 pm to 6:00 am. It can be seen that both experimental and CFD results have the same trend, where the value of heat transfer coefficient increases till reaches the highest value during the zone from 12:00 noon to 15:00 pm.

Figure 13 shows the variation of outer heat transfer coefficient from 9:00 pm to 6:00 am. Generally the results have the same trend compared with the inner heat transfer coefficient results. It can be noticed that the difference between experimental and CFD results has been improved compared with inner heat transfer coefficient. Some parameters are causing this improvement such as temperature difference and medium properties.
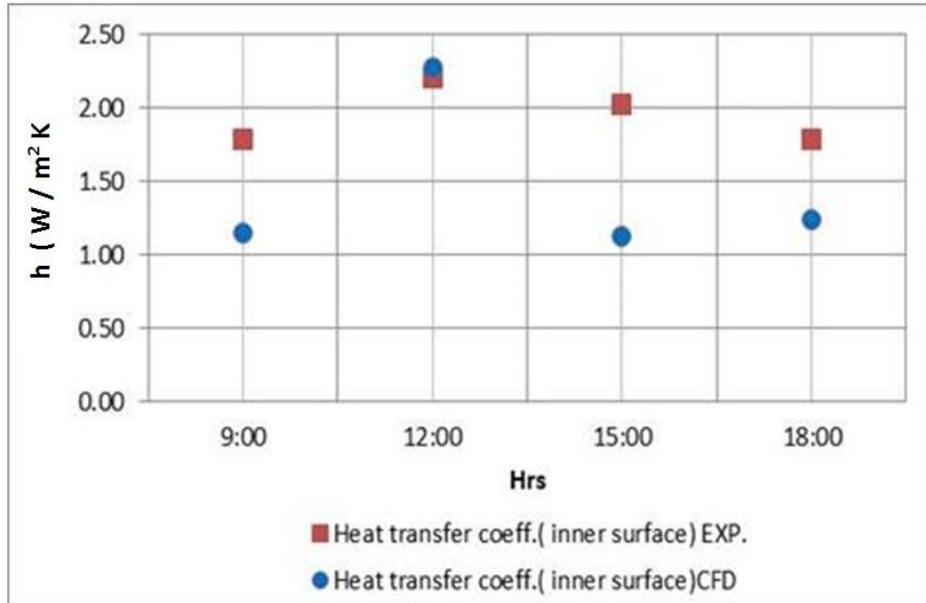
Figure 12. Variation of experimental and CFD of heat transfer coefficient (inner surface) with time
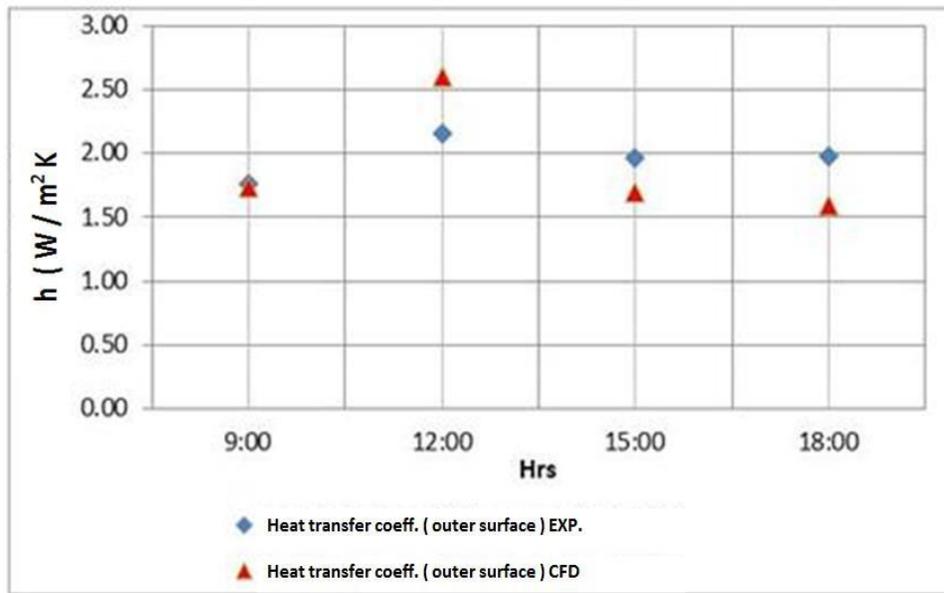
Figure 13. Variation of Experimental and CFD Heat Transfer Coefficient (Outer Surface) with Time

Figures 14 shows the comparison between inner and outer experimental heat transfer coefficients. The results explained that the values of experimental results of inner and

outer surface are very closed to each other. This means that temperature difference and physical properties of the flow between inner and outer surface are very closed.

Figures 15 shows the comparison between inner and outer CFD heat transfer coefficients. The deviation between inner and outer surface is bigger than that of the experimental values in figure 14. This figure shows that CFD program using constant fixed value i.e. flow properties, inside and outside air temperatures, while in reality or practically these parameters are changing from instant to other.
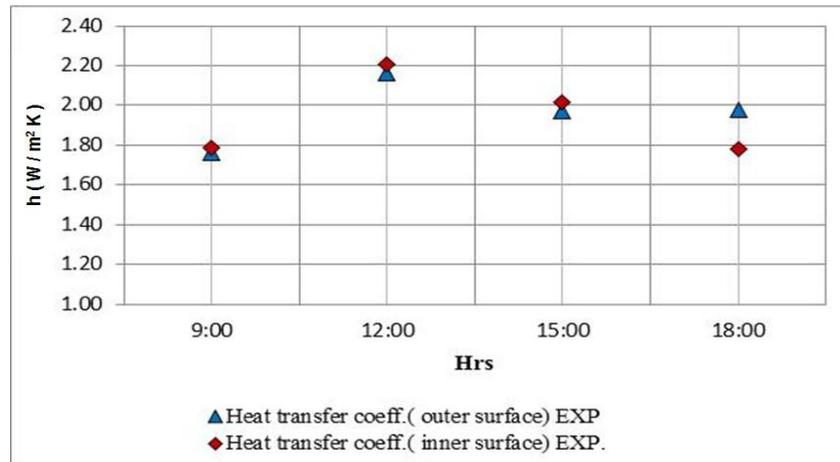
Figure 14. Comparison of experimental results of inner & outer surface heat transfer coefficient
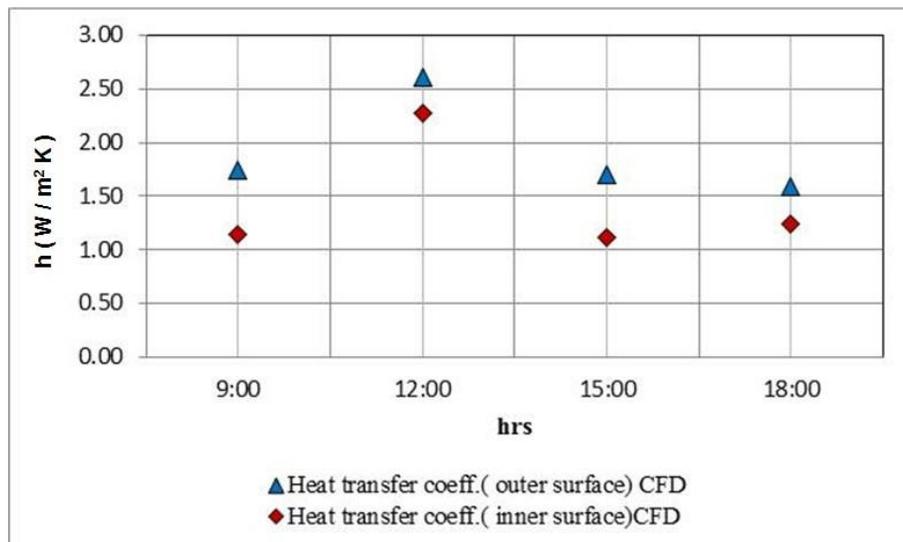
Figure 15. Comparison of CFD results of inner & outer surface heat transfer coefficient

6. Conclusions

 The air velocity and air temperature measurements were simulated and analyzed by numerical simulation for indoor environment in air conditioning office in desert climate. From the comparison of the CFD simulation with field measurement and results using the realizable k–ε, the following conclusions are drawn:

(1) The difference between the internal and external temperatures is almost constant during the day and varies from 9 °C to 14 °C.

(2) The internal temperature decreases with the increase of distance from the window.

(3) The CFD program has the same temperature profile trend as that achieve experimentally.

(4) The airflow velocity inside test office was low less than 0.3 m/s.

(5) The CFD program has good agreement with the experimental results. The maximum percentage error is 4.4%.

(6) The maximum temperature difference was 15 K obtained at 3 pm. The minimum temperature difference is 8 K obtained at 09:00 am.

(7) Experimental and CFD heat transfer coefficients during the day are increasing till reach the maximum values then starts decreasing again.

Acknowledgment

7. References

[1] Givoni, B. (1981). Man, Climate and Architecture, London: Applied Science Publishers
[2] ASHRAE 2001. 2001 ASHRAE handbook. Atlanta: American Society of Heating, Refrigerating and Air-Conditioning Engineers, Inc
[3] Pereira, F. O. R; Sharples, S. 1991. The development of a device for measuring solar heat gain and shading coefficients in scale models. Energy and Buildings 17: pp271-281
[4] Anderson JD. Computational fluid dynamics, International Edition, New York: McGraw-Hill; 1995

[5] Baker AJ, Richard MK, Eliott BG, Subrata Roy, Edward GS. Computational fluid dynamics: a two-edged sword. ASHRAE Journal 1997:51–8.

[6] K.W.D. Cheong ∗, E. Djunaedy, Y.L. Chua, K.W. Tham, S.C. Sekhar, N.H. Wong, M.B. Ullah, Thermal comfort study of an air-conditioned lecture theatre in the tropics, Building and Environment 38 (2003) 63 – 73

[7] María José Suárez, Antonio José Gutiérrez, Jorge Pistono, Eduardo Blanco CFD analysis of heat collection in a glazed gallery, Energy and Buildings, Volume 43, Issue 1, January 2011, Pages 108-116

[8] Jorge S. Carlos, Helena Corvacho, Pedro D. Silva, J.P. Castro-Gomes. Modelling and simulation of a ventilated double window, Applied Thermal Engineering, Volume 31, Issue 1, January 2011, Pages 93-102

[9] Kamal A.R. Ismail, Carlos T. Salinas, Jorge R. Henrique. A comparative study of naturally ventilated and gas filled windows for hot climates Energy Conversion and Management, Volume 50, Issue 7, July 2009, Pages 1691-1703

[10] Sujoy Pal, Biswanath Roy, Subhasis Neogi Heat transfer modelling on windows and glazing under the exposure of solar radiation Original Energy and Buildings, Volume 41, Issue 6, June 2009, Pages 654-661

[11] Ooi Yongsona, Irfan Anjum Badruddina,, Z.A. Zainala, P.A. Aswatha Narayanab 'Airflow analysis in an air conditioning room' Building and Environment 42 (2007) 1531-1537

[12] Sami A. Al-Sanea, M.F. Zedan, M.B. Al-Harbi Heat transfer characteristics in air-conditioned rooms using mixing air-distribution system under mixed convection conditions International Journal of Thermal Sciences, Volume 59, September 2012, Pages 247-259

[13] Murakami S, Kato S, Nakagawa H. Numerical prediction of horizontal non-isothermal 3-D jet in room based on the k-model. ASHRAE Transactions 1991; 97(1):38–48.

[14] H.B. Awbi, M.M. Nemri, Scale effect in room airflow studies, Energy and Buildings 14 (1990) 207-210.

[15] Jiang He, Akira Hoyano. Measurement and simulation of the thermal environment in the built space under a membrane structure, Building and Environment Volume 44, Issue 6, June 2009, Pages 1119–1127

[16] Huang H, Ooka R, Kato S. Urban thermal environment measurements and numerical simulation for an actual complex urban area covering a large district heating and cooling system in summer. Atmos Environ 2005;39:6362–75

[17] Tanimoto J, Hagishima A, Chimklai P. An approach for coupled simulation of building thermal effects and urban climatology. Energ Build 2004;36:781–93

[18] Zhai JZ, Chen YQ. Sensitivity analysis and application guides for integrated building energy and CFD simulation. Energ Build 2006;38:1060–8.

[19] Li X, Yu Z, Zhao B, Li Y. Numerical analysis of outdoor thermal environment around buildings. Build Environ 2005; 40:853-66.

[20] Clarke J.A. Energy simulation in building design, Adam Hilger Ltd.; 1985

[21] Institute for building environment and energy conservation (IBEC) SMASH for Windows Ver.2 user's manual; 2000 (in Japanese)

[22] Harayama K et al. Numerical study based on unsteady radiation and conduction analysis prediction of outdoor environment with unsteady coupled simulation of convection, part 1. J Archit Plan (Trans AIJ) 2002;556:99-106 (in Japanese).

[23] Kim T, Kato S, Murakami S. Indoor cooling/heating load analysis based on coupled simulation of convection, radiation and HVAC control. Building and Environment 2001; 36:901–8.

[24] Murakami S, Kato S, Kondo Y, Takahashi Y, Choi DH. Analysis of an indoor thermal environment using the CFD method (part 1), CFD solutions and its application to indoor models. Transactions of the Society of Heating, Air-conditioning and Sanitary Engineers of Japan 1995; 57:105–15 (in Japanese).

[25] Holman, J. P.2002. Heat Transfer. 9th Edition, Mc Graw Hill. New York.